Scientific Research Publishing

Journal of Applied Mathematics and Physics, 2023, 11, 3984-3999
https://www.scirp.org/journal/jamp
ISSN Online: 2327-4379
ISSN Print: 2327-4352

# Modeling of Mixed Convection in a Lid Driven Wavy Enclosure with Two Square Blocks Placed at Different Positions

**Sree Pradip Kumer Sarker[1*], Md. Mahmud Alam[1], Md. Jahirul Haque Munshi[2]**

[1]Department of Mathematics, Dhaka University of Engineering and Technology (DUET), Gazipur, Bangladesh
[2]Department of Mathematics, Hamdard University Bangladesh, Munshigonj, Bangladesh
Email: *pradip.duet@gmail.com, alamdr.mahmud@duet.ac.bd, drmunshi@hamdarduniversity.edu.bd

**How to cite this paper:** Sarker, S.P.K., Alam, Md.M. and Munshi, Md.J.H. (2023) Modeling of Mixed Convection in a Lid Driven Wavy Enclosure with Two Square Blocks Placed at Different Positions. *Journal of Applied Mathematics and Physics*, **11**, 3984-3999.
https://doi.org/10.4236/jamp.2023.1112255

**Received:** November 17, 2023
**Accepted:** December 24, 2023
**Published:** December 27, 2023



## Abstract

The purpose of this paper is to investigate the simulation of mixed convection in a lid-driven wavy enclosure with blocks positioned at various positions. This study also examined the impact of the longitudinal position of the heated block on heat transfer enhancement. The Galerkin weighted residual finite element method is employed to computationally solve the governing equations of Navier-Stokes, thermal energy, and mass conservation. The enclosure consists of two square heated blocks strategically placed at different heights—firstly, one set is closer to the bottom surface; secondly, one set is nearer to the middle area and finally, one set is closer to the upper undulating surface of the enclosure. The wavy top wall's thermal insulation, along with active heating of the bottom wall and blocks, generates a dynamic convective atmosphere. In addition, the left wall ascends as the right wall falls, causing the flow formed by the lid. The study investigates the impact of the Richardson number on many factors, such as streamlines, isotherms, dimensionless temperature, velocity profiles, and average Nusselt numbers. These impacts are depicted through graphical illustrations. In all instances, two counter-rotating eddies were generated within the cage. Higher rotating speed consistently leads to improved performance, irrespective of other characteristics. Furthermore, an ideal amalgamation of the regulating factors would lead to increased heat transmission.

## Keywords

Mixed Convection, Lid-Driven, Wavy Top Surface, and Square Heated Blocks

## 1. Introduction

The interaction between natural and forced convection in enclosed geometries is a crucial phenomenon that has significant ramifications in engineering and industrial processes. An enclosure driven by a lid is a specific configuration that has attracted interest due to its dynamic flow patterns caused by the movement of the surrounding walls. Comprehending and enhancing the process of heat transmission in these enclosures is of utmost importance for several applications, including the cooling of electronics and energy conversion devices. This study investigates the complex dynamics of mixed convection in a lid-driven enclosure with a top surface that has a wavy shape. The distinct wavy shape of the upper border intensifies the intricacy of the convective flow. In addition to this intricate nature, two heated square-shaped blocks are strategically placed inside the cage. The blocks are located in two separate configurations: first, one set is closer to the enclosure's bottom surface; next, one set is closer to the middle region; and last, one set is closer to the enclosure's upper, undulating surface. The strategic positioning of this component is expected to give the system unique thermal and flow properties.

The upper undulating barrier is identified as a thermal insulator, highlighting the primary influence of the lower barrier and heated blocks in propelling the convective movement. In addition, to enhance forced convection, the left wall is set to ascend, while the right wall descends. The coordinated movement of the enclosing walls creates a flow that is driven by the lid, adding another level of intricacy to the transfer of heat by convection. The investigation of mixed convection in constrained geometries has attracted considerable research attention due to its applicability in various engineering applications. Below, we will review a collection of important studies in this field:

Mahjabin and Alim [1] conducted a study on the influence of Hartmann number on the flow of magnetohydrodynamic (MHD) fluid in a square cavity with a heated cone of varying orientation. Their research yielded significant insights into the effects of magnetic fields. In their study, Senthil Kumar *et al.* [2] utilized a velocity-vorticity formulation in numerical simulations to investigate double diffusive mixed convection in a lid-driven square cavity. Their research provided valuable insights into the impact of velocity and vorticity fields. Ching *et al.* [3] utilized finite element simulations to investigate the combined convection of heat and mass movement in a right triangular enclosure, providing insight into the intricate flow dynamics occurring within these geometries. Hossain *et al.* [4] performed a finite element study to investigate the impact of magnetic fields on heat transfer properties in an open square cavity with a heated circular cylinder, focusing on MHD free convection flow.

Kumar *et al.* [5] performed a comprehensive examination of non-Darcy models for mixed convection in a porous cavity. They utilized a multigrid technique to study the flow and heat transfer characteristics. Jani *et al.* [6] conducted a study on magnetohydrodynamic free convection in a square cavity with bottom heating. Their research yielded significant findings on the interaction between magnetic fields and convective heat transfer. Rahman *et al.* [7] investigated the phenomenon of mixed convection flow in a rectangular vented cavity containing a heat-conducting square cylinder in its center. Their study aimed to enhance our comprehension of the flow patterns and temperature distributions in similar arrangements. Azizul *et al.* [8] observed heat lines in a double lid-driven cavity with a heated wavy wall, providing understanding of the complex heat transmission patterns related to mixed convection. In their study, Chamkha [9] examined the phenomenon of hydro-magnetic combined convection flow in a vertical cavity with a lid that is controlled by external forces. The study specifically focused on the influence of internal heat generation or absorption on the flow patterns, aiming to enhance our understanding of the interplay between magnetic and thermal processes.

Prasad and Koseff [10] investigated the heat transfer that occurs when both forced and natural convection are present in a deep hollow flow driven by a lid. Their study provided valuable insights into the complex nature of convective heat transfer in such enclosed spaces. Islam *et al.* [11] conducted an analysis of simulating natural convection flow with Magneto-Hydrodynamics in a wavy top enclosure featuring a semi-circular heater. Moreover, in a separate investigation, Munshi [12] examines the phenomenon of hydrodynamic mixed convection in a square cavity controlled by a moving lid. The study involves the presence of a heated block with an elliptical shape and a heater located at one of the corners. In their study, Munshi *et al.* [13] examined the optimization of mixed convection in a square hollow with porous walls and a lid-driven flow. The cavity also included an adiabatic block with an elliptic shape and linear side walls. Munshi *et al.* [14] conducted a study on the numerical simulation of mixed convection heat transfer of nanofluid in a square enclosure with a lid-driven porous medium. The investigations have utilized numerical approaches such as finite element methods [15] and [16], which have been highly beneficial for simulating and comprehending intricate convective fluxes.

The following sections are structured as follows: The geometric arrangement is outlined in Section 2. Section 3 presents a theoretical formulation to accurately define the situation. Section 4 is dedicated to the solution methodology. The program's validations are displayed in Section 5. The findings from the numerical simulations are displayed in Section 6. This section presents both qualitative fluid flow patterns and quantitative data, while also addressing consistence and convergence difficulties. Possible future works are included in Section 7. And, the paper concludes with a final statement in the Section 8.

## 2. Geometrical Configuration

The study examines the occurrence of mixed convection in a specifically built enclosure with unique geometric features and thermal boundary conditions. The enclosure is delineated **Figures 1(a)-(c)** by the subsequent parameters:

The enclosure is a square domain with specific length, width, and height measurements. The upper wall displays a unique undulating shape, resulting in an uneven surface profile for the enclosure. This wall is thermally insulated, meaning that it does not engage in the transfer of heat. The lower wall of the enclosure experiences uniform heating, which acts as a key source of thermal energy in the system. The left wall is designed to travel upwards, adding a dynamic element to the system. Additionally, it possesses thermal insulation properties, which implies that it does not directly engage in the heat transfer mechanism. Unlike the left wall, the right wall descends, which adds to the system's dynamic

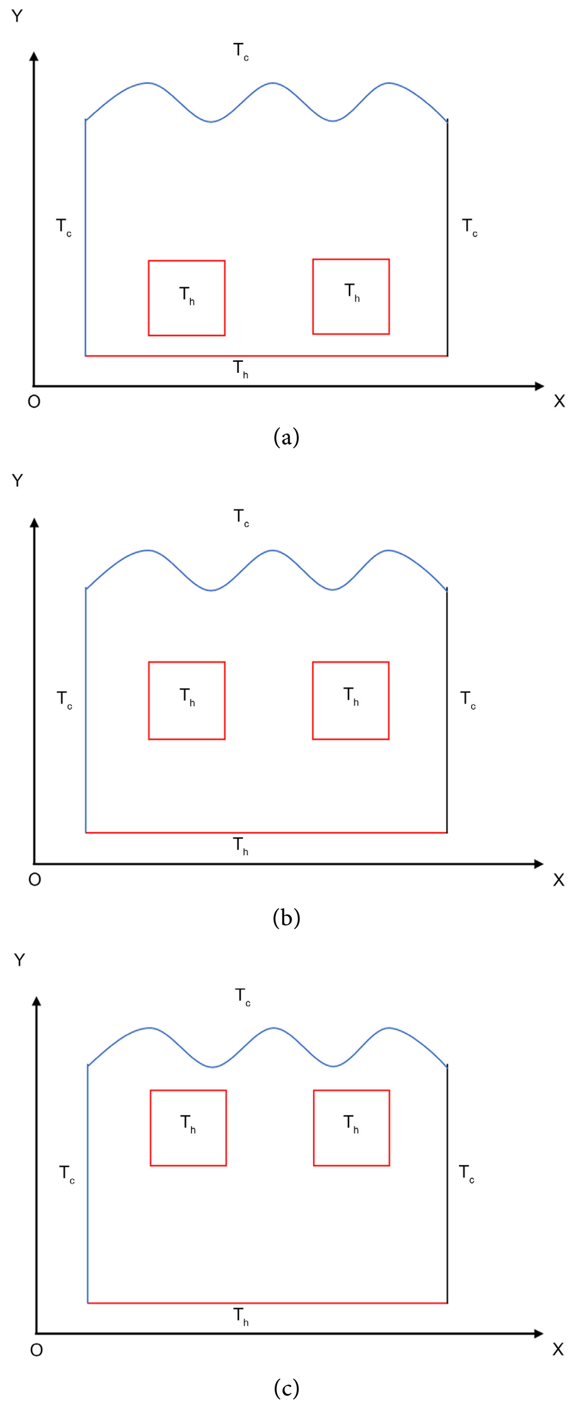


**Figure 1.** (a) (b) (c): Schematic diagram of the investigated lid-driven wavy enclosure with block in different locations. (a) Bottom Position (b) Middle Position and (c) Top Position.

nature. The right wall, like the left wall, is thermally insulated. Two square blocks are positioned inside the enclosure, and their placement differs for the three different scenarios being studied. In the first situation, the two square blocks are positioned closer to the bottom of the enclosure. In the second situation, the two square blocks are located closer to the center of the enclosure. In the third situation, the two square blocks are positioned closer to the upper wavy enclosure. Each of these blocks undergoes uniform heating, serving as supplementary heat sources within the system.

## 3. Mathematical Formulation

The mathematical formulation for the investigation of mixed convection in the specified enclosure encompasses the conservation equations for mass, momentum, energy, as well as the equations that reflect the boundary conditions. Considering the intricate nature of the situation, let us analyse the fundamental equations pertaining to the dimensions involved:

$$\frac{\partial u}{\partial x}+\frac{\partial v}{\partial y}=0$$

$$u\frac{\partial u}{\partial x}+\frac{\partial u}{\partial y}=-\frac{1\partial p}{\rho\partial x}+v\left(\frac{\partial^2 u}{\partial x^2}+\frac{\partial^2 u}{\partial y^2}\right)$$

$$u\frac{\partial v}{\partial x}+v\frac{\partial v}{\partial y}=-\frac{1\partial p}{\rho\partial y}+v\left(\frac{\partial^2 v}{\partial x^2}+\frac{\partial^2 v}{\partial y^2}\right)+g\beta\left(T-T_c\right)$$

$$u\frac{\partial T}{\partial x}+v\frac{\partial T}{\partial y}=\alpha\left(\frac{\partial^2 T}{\partial x^2}+\frac{\partial^2 T}{\partial y^2}\right)+\frac{Q_0\left(T-T_c\right)}{\rho C_p}$$

Dimensional boundary conditions:

Top wavy wall: $u=v=0, T=T_c, 0\le x\le L, y=\frac{L}{2}\left(1+\sin 2n\pi x\right)$

Bottom wall: $u=v=0, T=T_h, 0\le x\le L$

Left wall: $u=v=0, \frac{\partial T}{\partial x}=0, 0\le y\le\frac{L}{2}$

Right wall: $u=v=0, \frac{\partial T}{\partial x}=0, 0\le y\le\frac{L}{2}$

The equations are dimensional by using the following dimensionless parameters

$$X=\frac{x}{L}, Y=\frac{y}{L}, U=\frac{u}{U_0}, V=\frac{v}{U_0}, P=\frac{p}{\rho U_0^2}, \theta=\frac{T-T_c}{T_h-T_c}$$

$$Pr=\frac{\nu}{\alpha}, Re=\frac{VL}{\nu}, Gr=\frac{g\beta\left(T_h-T_c\right)L^3}{\nu^2}, Ri=\frac{Gr}{Re^2}, \nu=\frac{\mu}{\rho}$$

In this context, $X$ and $Y$ represent dimensionless coordinates that fluctuate horizontally and vertically, respectively. U and V represent dimensionless velocity components in the $X$ and $Y$ directions, respectively. $\theta$ represents the temperature without units, $P$ represents the pressure without units, and $Q$ represents the heat generation parameter. *Re*, *Pr*, *Gr*, and *Ri* are the Reynolds number, Prandtl's number, Grashof number, and Richardson number correspondingly.

The dimensionless governing equations:

$$\frac{\partial U}{\partial x}+\frac{\partial V}{\partial Y}=0$$

$$U\frac{\partial U}{\partial x}+V\frac{\partial V}{\partial Y}=-\frac{\partial P}{\partial X}+\frac{1}{Re}\left(\frac{\partial^2 U}{\partial X^2}+\frac{\partial^2 U}{\partial Y^2}\right)$$

$$U\frac{\partial U}{\partial x}+V\frac{\partial V}{\partial Y}=-\frac{\partial P}{\partial Y}+\frac{I}{Re}\left(\frac{\partial^2 U}{\partial X^2}+\frac{\partial^2 U}{\partial Y^2}\right)+Ri\theta$$

$$U\frac{\partial \theta}{\partial x}+V\frac{\partial \theta}{\partial Y}=\frac{1}{RePr}\left(\frac{\partial^2 \theta}{\partial X^2}+\frac{\partial^2 \theta}{\partial Y^2}\right)+Q\theta$$

Dimensionless boundary conditions:

Top wavy wall: $U=V=0, \theta=0$

Bottom wall: $U=V=0, \theta=1$

Left wall: $U=V=0, \frac{\partial \theta}{\partial N}=0$

Right wall: $U=V=0, \frac{\partial \theta}{\partial N}=0$

The Richardson number is a crucial metric for analysing the phenomenon of mixed convection. When $Ri$ = 1, it indicates that the case is purely convection. When the Richardson number is low ($Ri$ < 1), the flow is primarily influenced by viscous force, and might be considered to be aided by forced convection. However, when the Richardson number exceeds 1 ($Ri$ > 1), the buoyancy force prevails over the viscosity force, causing the fluid to flow due to natural convection. In 1883, Osborne Reynolds conducted a straightforward experiment that confirmed the presence of two distinct types of flows. A flow is considered laminar when the Reynolds number ($Re$) is less than 2000, while it is considered turbulent when $Re$ is greater than 4000. A Reynolds number ranging from 2000 to 4000 signifies the shift from a smooth, orderly flow (laminar) to a chaotic, irregular flow (turbulent).

The heat transfer coefficient in terms of local Nusselt number $Nu$ is defined by,

$$Nu=-\frac{\partial \theta}{\partial \eta},$$

where $\eta$ is the outward drawn normal on the plane.

Dimensionless normal temperature gradient can be written as:

$$\frac{\partial \theta}{\partial \eta}=\sqrt{\left(\frac{\partial \theta}{\partial X}\right)^2+\left(\frac{\partial \theta}{\partial Y}\right)^2}$$

While the average Nusselt number $\overline{Nu}$ is obtained by integrating the local Nusselt number along the bottom surface of wavy enclosure and is defined by

$$\bar{N}_u=-\frac{1}{L}\int_0^L \frac{\partial \theta}{\partial \eta}\mathrm{d}s$$

where $\theta$ is the dimensionless coordinate along the circular surface. If $L$ = 1 for length of the enclosure then,

$$\bar{N}_u = -\int_0^L \frac{\partial\theta}{\partial\eta} ds .$$

## 4. Numerical Technique

The nondimensionalized version of my physical problem is derived from the dimensional governing equations. Numerical solutions are obtained for the governing equations and boundary conditions using the Galerkin-Weighted Residual formulation and the finite element method [15]. The stated criteria are employed to guarantee that all dependent variables inside the solution domain achieve the objective of convergence.

$$\sum \left| \phi_{i,j}^{n} - \phi_{i,j}^{n-1} \right| \le 10^5$$

where $\phi$ represents the dependent variables $U$, $V$, $P$ and $T$ the indexes $i$, $j$ refers to space coordinates and the index $n$ is the current iteration.

## 5. Validation of a Program

**Figure 2** depicts the distinction between streamlines and isotherms in the graphical solution. The numerical data unequivocally demonstrates a high degree of concurrence between the two outcomes.

## 6. Results and Discussions

Simulating mixed convection in a lid-driven wavy enclosure with a block placed at various points has provided useful insights into the intricate flow and heat transmission properties of the system. The results have been obtained for the Richardson number, which varies between 0.01 and 5. The results are displayed in the form of streamlines and isotherms within various sections of the enclosure block. The figures depict the changes in streamlines and isotherms within the enclosure as the Richardson number varies. **Figure 3** displays the variations in streamlines, while **Figure 4** illustrates the changes in isotherms. The subsequent significant discoveries are given alongside an exhaustive analysis.

The placement of the heated blocks is crucial in determining the flow patterns and temperature distributions inside the enclosure. In **Figure 3(a)**, the blocks are located closer to the bottom of the cage. The streamlines clearly indicate the formation of a pair of counter rotating eddies within the cage. Furthermore, there is a documented occurrence of limited upward flow along the undulating surface. The occurrence of this phenomena can be ascribed to the combined influence of buoyancy-driven flow and the obstructive presence of the blocks. In contrast, **Figure 3(b)** demonstrates a more uniformly dispersed flow when the blocks are positioned closer to the center of the enclosure. The streamlines in **Figure 3(c)** clearly show the formation of a pair of counter-rotating eddies in the vicinity of the lower edge of the enclosure. Analysis of the streamlines reveals that when the Richardson number increases, the centers of rotating eddies shift upwards and closer to the upper boundary of the enclosure.

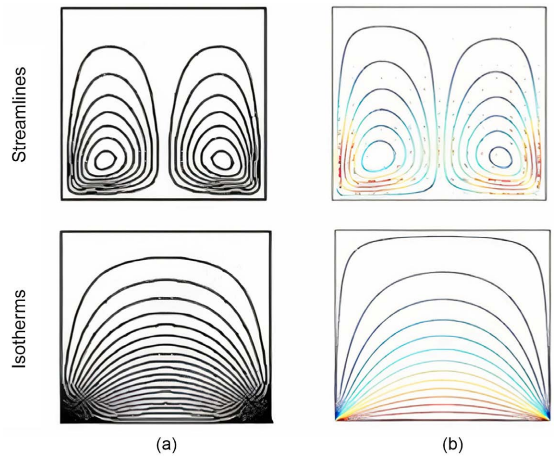


**Figure 2.** Comparison between streamlines and isotherms for graphical solution of (a) Jani *et al.* [6] and (b) Present study at $Ra = 10^4$ and $Ha = 50$.

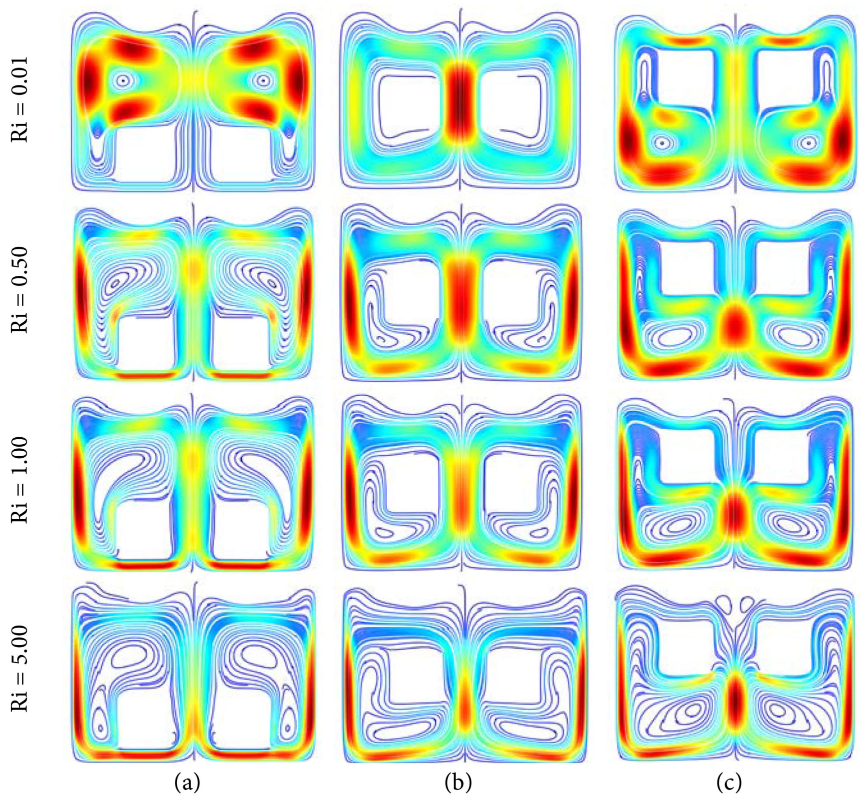


**Figure 3.** Streamlines for different values of Richardson number with block in different locations while $Pr = 0.71$, $Gr = 10^4$ and $Re = 100$. (a) Bottom (b) Middle (c) Top.

The undulating upper surface of the wall functions as a thermal insulator, impeding the transmission of heat by conduction. This has a substantial impact on the thermal distribution within the container. The presence of wavy geometry leads to the emergence of additional intricacies, which in turn give rise to the development of clearly defined thermal boundary layers and areas of recirculation. The presence of these characteristics leads to an uneven distribution of temperature, especially in the area surrounding the undulating surface.

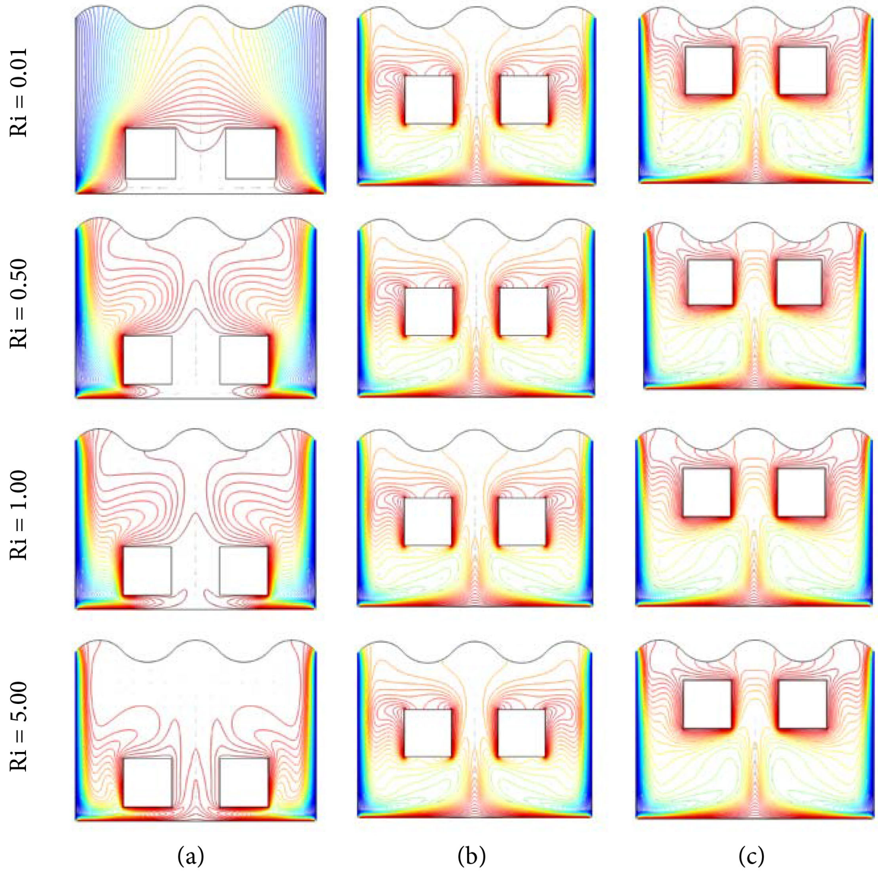


**Figure 4.** Isotherms for different values of Richardson number with block in different locations while $Pr = 0.71$, $Gr = 10^4$ and $Re = 100$. (a) Bottom (b) Middle (c) Top.

**Figure 4** demonstrates the prevalence of heat transport governed by the prevailing conditions, as indicated by the isotherms. The isotherms in **Figure 4(a)** exhibit parallel alignment with the center walls of the enclosure when the Richardson number is at its minimum value, indicating minimal convective heat transport. In alternative realms, **Figure 4(b)** and **Figure 4(c)** illustrate the isotherm lines along the side walls. These lines demonstrate the strengthening of the moving lid and the decrease in heat transfer by convection, as indicated by different values of the Richardson number. As the Richardson number grows, there is a greater curvature in the isotherms around the obstruction, which suggests a higher level of heat transfer through convection. These findings provide insight into the intricate relationship between the flow and heat transfer properties within the enclosure, emphasizing the significant influence of the Richardson number on the rate of heat transfer.

**Figure 5** depicts the variations in velocity components along a vertical line for various Darcy number values. The graph demonstrates a positive correlation between the Darcy number and both the upper and lower limits of the velocity. Put simply, larger Darcy numbers result in greater maximum and minimum velocities along the vertical axis. This discovery suggests that the Darcy number exerts a substantial influence on the fluid's velocity distribution.

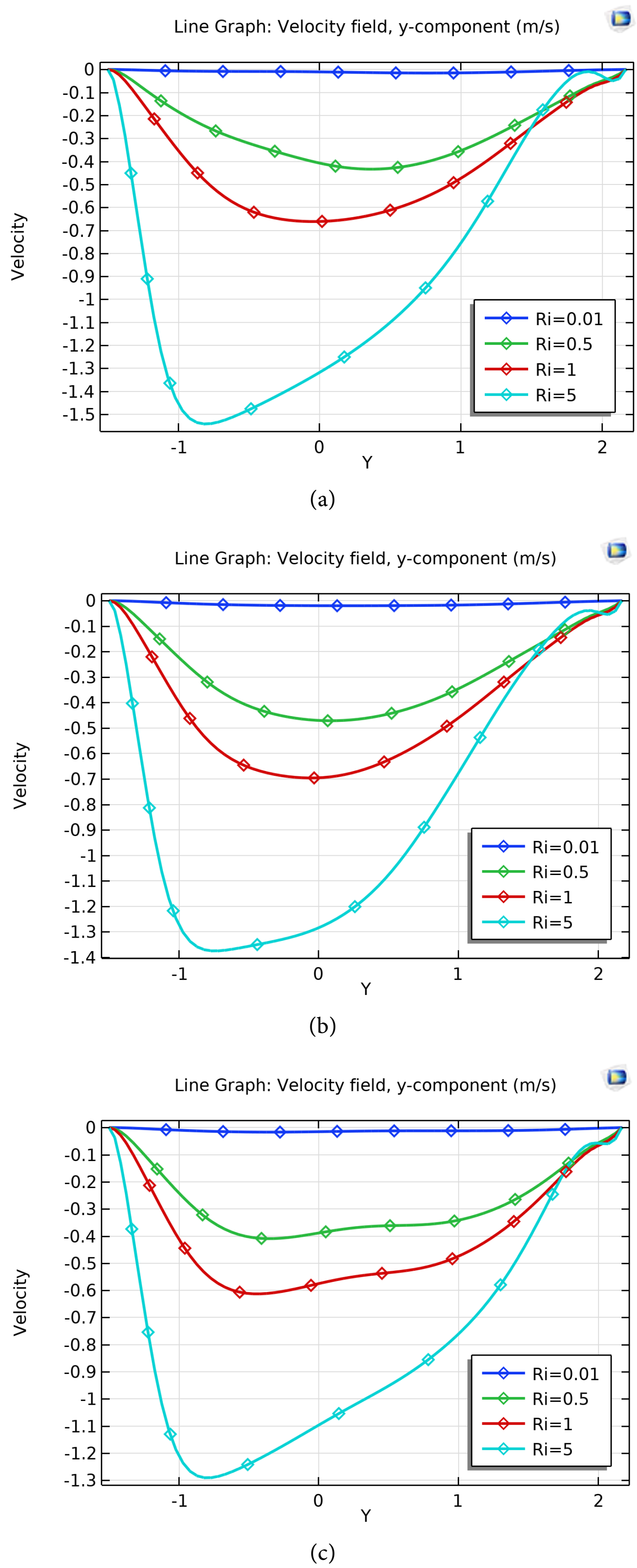


**Figure 5.** Variation of velocity profiles along *Y*-axis for different values of Richardson number with block (a) Bottom Position (b) Middle Position and (c) Top Position while $Pr = 0.71$, $Gr = 10^4$ and $Re = 100$.

The vertical velocity component of the enclosure is depicted in **Figure 5**, showcasing its fluctuations over different Richardson values. The graphic illustrates that the magnitude of the highest and lowest velocity values increases as the Richardson number increases.

**Figure 6** illustrates the variance of dimensionless temperature variations along the Y-axis of the enclosure for various Richardson values. The graph demonstrates a positive correlation between the Richardson numbers and the absolute values of both the maximum and minimum temperatures. Nevertheless, it is important to acknowledge that the rate of temperature change decelerates as the Richardson numbers increase. Put simply, larger Richardson numbers lead to more gradual temperature variations along the Y-axis of the enclosure. This discovery emphasizes the impact of Richardson numbers on the temperature distribution inside the fluid, indicating that larger Richardson numbers result in a more gradual temperature shift down the Y-axis.

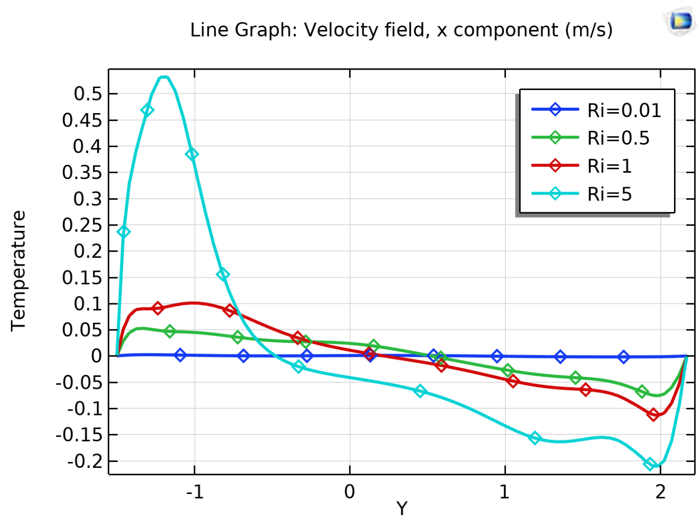


(a)

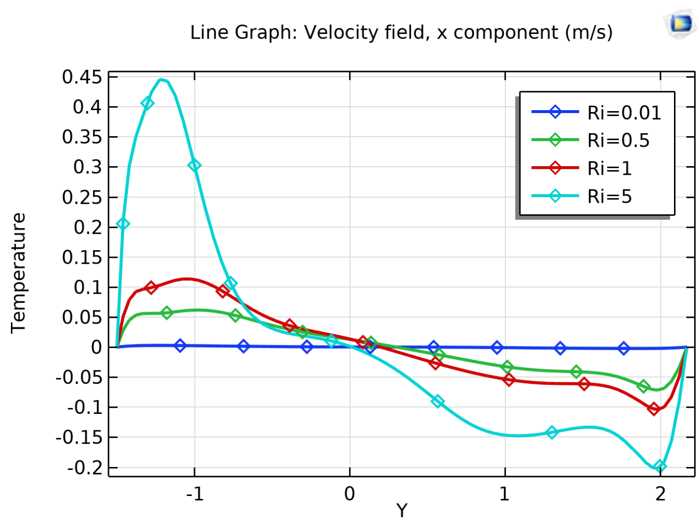


(b)

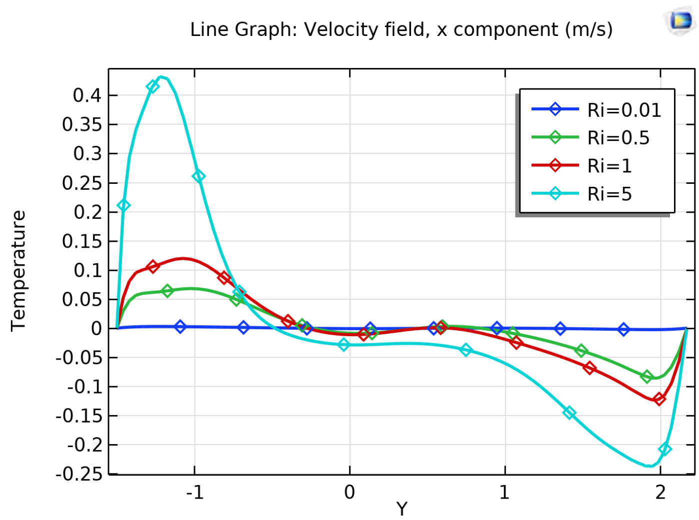


(c)

**Figure 6.** Variation of dimensionless temperature along *Y*-axis for different values of Richardson number with block (a) Bottom Position (b) Middle Position and (c) Top Position while $Pr = 0.71$, $Gr = 10^4$ and $Re = 100$.

**Figure 7** illustrates the relationship between the local Nusselt number and various Richardson numbers. The data suggests that when the buoyancy ratio and Richardson numbers increase, there is a corresponding increase in heat transmission. This occurs due to the presence of a stagnation point, which is the position where the fluid's velocity reaches zero. Consequently, the highest rate of heat transfer is achieved at this specific spot. To summarize, the graph illustrates that the local Nusselt number is affected by multiple factors, but the most heat transmission happens at the stagnation point, which is located at this particular position.

## 7. Possible Future Works

While the present study has provided valuable insights into the complexities of mixed convection in a lid-driven wavy enclosure with strategically placed square heated blocks, there are several avenues for future research that can build upon the current findings and address certain limitations:

- Exploration of Additional Geometries
- Incorporation of Variable Wavy Geometries
- Optimization of Block Placement
- Effect of Block Materials
- Parametric Studies on Buoyancy and Lid Movement
- Analysis of Transient Effects
- Inclusion of Nanofluids
- Experimental Validation
- Study of Multi-Physics Phenomena
- Environmental and Industrial Applications

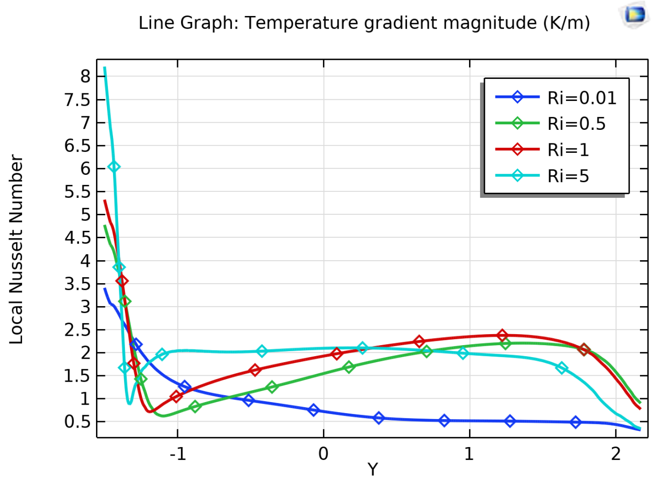


(a)

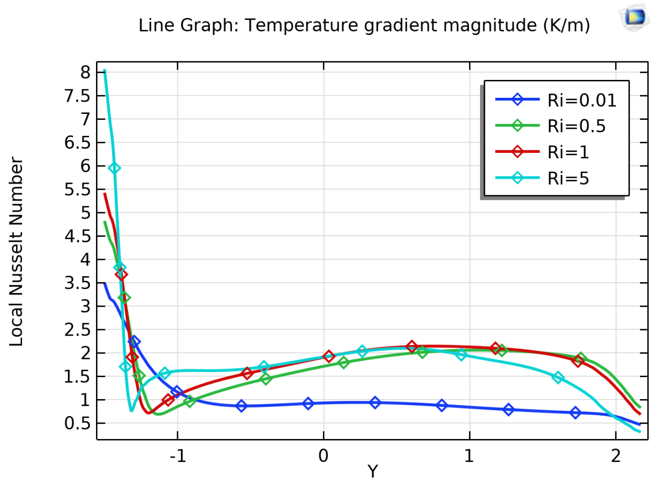


(b)

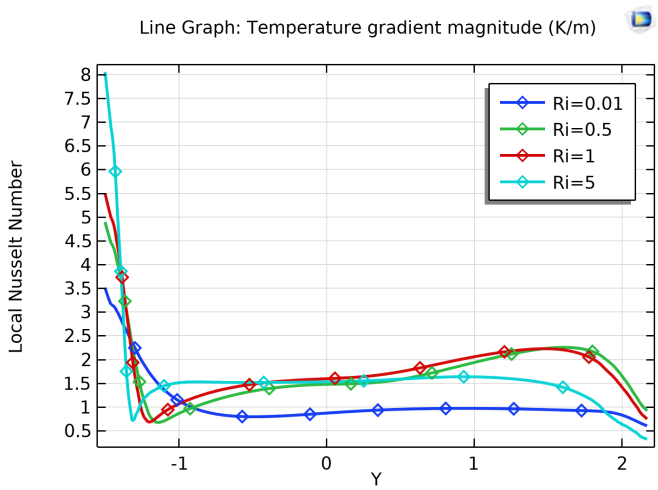


(c)

**Figure 7.** Variation of local Nusselt number along *Y*-axis for different values of Richardson number with block (a) Bottom Position (b) Middle Position and (c) Top Position while $Pr = 0.71$, $Gr = 10^4$ and $Re = 100$.

Finally, future research should aim to expand the current understanding of mixed convection in wavy enclosures by exploring diverse geometries, optimizing system parameters, and considering real-world applications. Addressing these areas will contribute to the advancement of knowledge in convective heat transfer and foster practical innovations in engineering and technology.

## 8. Conclusions

This study examined the complexities of mixed convection in a lid-driven enclosure with a wavy top wall and heated square blocks placed at different heights. The enclosure exhibited certain boundary conditions, which consisted of side walls with thermal insulation, a bottom wall that was heated, and a top wall with a wavy shape. In addition, the left wall had an upward trajectory while the right wall descended, resulting in a distinctive flow environment.

The arrangement of the heated blocks was a critical determinant of the flow patterns and temperature distributions inside the enclosure. When the blocks were positioned closer to the upper wavy case, a concentrated upward flow along the undulating surface was seen. In contrast, placing the blocks closer to the middle and bottom of the enclosure resulted in a more uniformly spread flow, leading to a more consistent distribution of temperature. The undulating upper wall, functioning as a thermal insulator, had a substantial impact on the temperature distribution within the enclosure. The introduction of the wavy geometry resulted in the emergence of intricate thermal boundary layers and areas of recirculation. The counteracting movements of the lateral walls generated supplementary vortical formations inside the enclosure, resulting in areas characterized by intense velocity differentials and turbulence. This had a further impact on both the patterns of fluid movement and the distribution of temperature. The application of heat to the lower wall and the blocks generated buoyancy forces that propelled the convective flow. The increased temperature of the lower wall caused a rising column of heated fluid, which affected the overall flow patterns. Moreover, the existence of heated blocks caused the formation of localized convection cells, leading to distinct fluctuations in temperature and velocity in those areas.

The heat transfer performance of the system was evaluated using quantitative metrics such as the Nusselt number, local heat transfer coefficients, and temperature gradients. The measurements offered significant data for assessing the effectiveness of the enclosure for particular applications.

To summarize, this work provides insight into the complex interaction between flow and heat transfer phenomena in the described enclosure arrangement. The knowledge acquired from this analysis establishes a strong basis for future research focused on enhancing the design of comparable enclosures for other engineering purposes. The proposed findings enhance the existing knowledge in the subject of convective heat transfer and have possible implications for designing systems in different industrial and environmental settings.

## Conflicts of Interest

The authors declare no conflicts of interest regarding the publication of this paper.

## References

[1] Mahjabin, S. and Alim, M.A. (2018) Effect of Hartmann Number on Free Convective Flow of MHD Fluid in a Square Cavity with a Heated Cone of Different Orientation. *American Journal of Computational Mathematics*, **8**, 314-325. https://doi.org/10.4236/ajcm.2018.84025

[2] Kumar, D.S., Murugesan, K. and Thomas, H.R. (2008) Numerical Simulation of Double Diffusive Mixed Convection in a Lid-Driven Square Cavity Using Velocity-Vorticity Formulation. *Numerical Heat Transfer A*, **54**, 837-865. https://doi.org/10.1080/10407780802424213

[3] Ching, Y.C., Öztop, H.F., Rahman, M.M., Islam, M.R. and Ahsan, A. (2012) Finite Element Simulation of Mixed Convection Heat and Mass Transfer in a Right Triangular Enclosure. *International Journal of Heat and Mass Transfer*, **39**, 689-696. https://doi.org/10.1016/j.icheatmasstransfer.2012.03.016

[4] Hossain, S.A., Alim, M.A. and Saha, S.K. (2015) A Finite Element Analysis on MHD Free Convection Flow in Open Square Cavity Containing Heated Circular Cylinder. *American Journal of Computational Mathematics*, **5**, 41-54. https://doi.org/10.4236/ajcm.2015.51003

[5] Kumar, D.S., Dass, A.K. and Dewan, A. (2009) Analysis of Non-Darcy Models for Mixed Convection in a Porous Cavity Using a Multigrid Approach. *Numerical Heat Transfer*, **56**, 685-708. https://doi.org/10.1080/10407780903424674

[6] Jani, S., Mahmoodi, M. and Amini, M. (2013) Magnetohydrodynamic Free Convection in a Square Cavity Heated from Below and Cooled from Other Walls. *International Journal of Mechanical*, *Aerospace*, Industrial, *Mechatronic and Manufacturing Engineering*, **7**, 750-755.

[7] Rahman, M.M., Elias, M., and Alim, M.A. (2009) Mixed Convection Flow in a Rectangular Ventilated Cavity with a Heat-Conducting Square Cylinder at the Center. *Journal of Engineering and Applied Sciences*, **4**, 20-29.

[8] Azizul, F.M., Alsabry, A.I., Hashim, I. and Chamkha, A.J. (2020) Heatline Visualization of Mixed Convection inside Double Lid-Driven Cavity having Heated Wavy Wall. *Journal of Thermal Analysis and Calorimetry*, **145**, 3159-3176. https://doi.org/10.1007/s10973-020-09806-5

[9] Chamkha, A.J. (2002) Hydromagnetic Combined Convection Flow in a Vertical Lid-Driven Cavity with Internal Heat Generation or Absorption. *Numerical Heat Transfer*. *Part A*, **41**, 529-546. https://doi.org/10.1080/104077802753570356

[10] Prasad, A.K. and Koseff, J.R. (1996) Combined Forced and Natural Convection Heat Transfer in a Deep Lid-Driven Cavity Flow. *International Journal of Heat and Fluid Flow*, **17**, 460-467. https://doi.org/10.1016/0142-727X(96)00054-9

[11] Islam, M.M., Alim, M.A., Alam, M.M. and Munshi, M.J.H. (2023) Simulation of Natural Convection Flow with Magneto-Hytrodynamics in a Wavy Top Enclosure with a Semi-Circular Heater. *Open Journal of Applied Sciences*, **13**, 591-603. https://doi.org/10.4236/ojapps.2023.134047

[12] Munshi, M.J.H., Alim, M.A., Bhuiyan, A.H. and Ali, M. (2017) Hydrodynamic Mixed Convection in a Lid-Driven Square Cavity Including Elliptic Shape Heated Block with Corner Heater. *American Institute of Physics* (*AIP*), **194**, 442-449.

https://doi.org/10.1016/j.proeng.2017.08.169

[13] Munshi, M.J.H., Alim, M.A., Bhuiyan, A.H. and Ali, M. (2017) Optimization of Mixed Convection in a Lid-Driven Porous Square Cavity with Internal Elliptic Shape Adiabatic Block and Linearly Heated Side Walls. *American Institute of Physics* (*AIP*), **1851**, Article ID: 020049. https://doi.org/10.1063/1.4984678

[14] Munshi, M.J.H., Alim, M.A., Bhuiyan, A.H. and Ahmed, K.F.U. (2019) Numerical Simulation of Mixed Convection Heat Transfers of Nanofluid in a Lid-Driven Porous Medium Square Enclosure. *American Institute of Physics* (*AIP*), **2121**, Article ID: 030005. https://doi.org/10.1063/1.5115850

[15] Reddy, J.N. (1993) An Introduction to Finite Element Method. McGraw-Hill, New York.

[16] Zienkiewicz, O.C. and Taylor, R.L. (1991) The Finite Element Method. 4th Edition, McGraw-Hill, New York.